Seismic vs. geodetic moments at Mt. Etna volcano: a tool for a rapid understanding the eruptive behaviour?

Salvatore Gambino*, Giovanni Distefano°, Vincenza Maiolino*, Stefano Gresta°

*Istituto Nazionale di Geofisica e Vulcanologia, Sezione di Catania, P.zza Roma 2, 95123 Catania, Italy

°Dipartimento di Scienze Biologiche, Geologiche e Ambientali, Università degli Studi di Catania, Corso Italia 57 95129 Catania, Italy

Submitted to JVGR (Short Communication)

Revised Version (October 2018)

Correspondence to:

Salvatore Gambino
Istituto Nazionale di Geofisica e Vulcanologia
Sezione di Catania Osservatorio Etneo
P.zza Roma 2, 95123 Catania, Italy
Tel: 39-957165877
e-mail: salvatore.gambino@ingv.it

Abstract

The seismic to geodetic moment ratio (M_o/M_G) related to seven magma intrusion episodes, occurring at Mt. Etna volcano between 1981 and 2008, are considered.

The lateral eruptions show a moment ratio of 0.04-0.06; meaning that only about 5% of the stress energy accumulated with ground deformation was released by earthquakes. Significantly higher values instead characterized vertical (0.25-0.50) and non-eruptive (0.17) dike intrusions.

This paper proposes a simple relationship, in order to estimate, during the early phases of an eruption, the intruding magma volumes by the cumulative seismic moment (of the ongoing seismicity) and elapsed time.

Keywords*: seismic swarms; intrusion; stress rate; magma.*

1.0 Introduction

Mount Etna is a large basaltic volcano formed in a geodynamic setting generated during the Neogene convergence between the African and European plates (Fig. 1; e.g. Allard et al., 2006).

It's located between the compressive domain of Western-Central Sicily and the tensional domain of the Calabrian Arc; it has formed at the intersection of two regional fault systems, trending NNW-SSE and NE-SW (e.g. Lo Giudice et al., 1982), respectively (MF and ME in Fig. 1).

Mount Etna is characterized by persistent activity (degassing and Strombolian activity) and lateral flank eruptions that occur when a magma-driven fracture (usually a dike) propagate from the source to the surface.

Ground deformation provided essential information allowing, by data inversion, to obtain dike geometry and identify magma transport within the volcano edifice. A primary source, commonly applied in dike modeling, is the rectangular tensile dislocation (e.g. Okada, 1985).

The dike propagation process may change the stress field in the rock volume around the intrusion, causing earthquake swarms that generally occur ahead of the dike tip, above it and in the regions adjacent to the dike walls (e.g. Toda et al. 2002).

A parameter linking deformation and seismicity in a given area is the seismic to geodetic moment ratio (M_o/M_G) that gives a proportion of the stress energy accumulated through deformation of the crust that is released by seismicity. This value multiplied by 100 and expressed as a percentage represents the seismic efficiency (e).

The awareness of the M_o/M_G for a volcano may be useful in order to estimate magma volumes from seismicity that is being recorded.

However, Pedersen et al. (2007), considering three different areas in Iceland, showed how the relationship between volume change and resulting seismicity varies greatly among cases: the stressing rate is not a dominating factor for occurrence of magmatically induced seismicity while the main factor controlling the level of seismic energy release seems to be the background seismicity rate in the intruded area (Pedersen et al., 2007). Therefore intrusion into a relatively stable area, generally produces low seismic energy release while high M_o/M_G values characterize intruded areas with high tectonic activity and regional stress.

For a specific area, intrusion depth and typology or local inhomogeneity in geological-structural features may be the cause of different moment ratios.

On Mt. Etna, persistent activity at summit craters varies from degassing to Strombolian activity, until to lava fountains. Flank eruptions represent the final step of magma intrusion processes and may be defined as lateral and eccentric. The former occur when the dike propagates both vertically and laterally, from the source to the surface encompassing the central magma feeding system.. Eccentric eruptions are due to dikes mainly vertically uprising, independently from the central magma feeding system.

Mount Etna is one of the best monitored volcanoes in the world. Seismic and ground deformation data have been collected continuously at permanent stations for about 50 years.

In this study the seismic to geodetic moment ratio (M_o/M_G) on Mt. Etna is analysed, by considering seven dike intrusion episodes. These episodes, thanks to robust seismic and geodetic datasets are characterized by one (or more) source models referred to in current literature.

2.0 Instrumental networks

2.1 Seismic network

Systematic instrumental investigations of seismic activity at Mt. Etna roughly began at the end of 1960's by a seismic permanent network by the Catania University made up of 11 one-component vertical stations (Gresta & Patanè, 1987). Since the end of the 1980's, the network was managed by the IIV-CNR that installed three-component stations. The resulting network was formed by 13 stations (11 equipped with short-period 1 s sensors and 2 equipped with broadband 10 s sensor) and all stations were linked in real time by radio and cable to the data acquisition centre in Catania where the signals were automatically analysed and stored (Patanè et al., 2004).

In 1994, a latter permanent network consisting in 44 stations was set up on the volcano, in the framework of the Poseidon Project. The networks by IIV-CNR and the Poseidon Project were then merged in 2001, into the newly created INGV.

At present, the Etna Seismic Network managed by INGV-Catania (INGV-CT) comprises about 40 stations (Fig. 1b) which allow continuous recording of data using broadband and short period seismometers.

2.2 Ground deformation networks

Ground deformations on Mt. Etna are measured by using different geodetic techniques such as EDM/GPS, and levelling discrete measurements, tilt and GPS continuous recording, and the DInSAR technique. Separately or jointly, they are a powerful tool to infer position and dimensions of magma dike intrusions.

2.2.1. Discrete measurements

Discrete measurements (EDM, GPS and levelling, Fig.1b) have been repeated systematically since the end of the 1970's. Three EDM networks were established during the early 1980s, closely corresponding to the northeast, south and western rifts that affect the volcano. Each network consists of about 14 to 16 geodetic benchmarks and a total of 36 to 47 lines, and has commonly been surveyed once per year (Neri et al., 2005). The levelling network was installed in 1980 and consist of ca. 200 benchmarks (Obrizzo et al., 2001) and since the 1990s a GPS-network that consists of 46 benchmarks, organized in three sub networks, is measured periodically (at least once a year) (Puglisi et al., 2008).

2.2.2. Continuous measurements

Tilt data represent the first continuous ground deformation records on Mt. Etna carried out since the 1970s with few stations able to record changes during the 1980's eruptions (Gambino et al., 2014).

Since 1991, the tilt network allowed a good areal coverage of Mt. Etna (Bonaccorso & Gambino, 1997). At present it consists of 16 bi-axial instruments and one fluid long-base. Almost all the bore-hole stations are 10-30 meters depth and are equipped with high resolution (<0.005 microradians) self-levelling instruments (Ferro et al., 2011).

In November 2000 the ground deformation continuous monitoring was upgraded with the installation of a permanent GPS network (Fig. 1b), that actually is made up of about 35 stations (e.g. Aloisi et al., 2011). CGPS data collected by this network are processed with the GAMIT/GLOBK method to produce constrained solutions.

3.0 Methodology

Seven intrusion episodes linked to six eruptions that occurred over the last 40 years on Mt. Etna (1981, 1989, 1991-93, 2001, 2002, 2008) are considered. The 2002 was a double eruption with a radial dike on the north-eastern slope of the volcano, and a vertical uprising dike on the southern flank, therefore we considered two cases named 2002NE and 2002S, respectively. For all these episodes, reliable seismicity analyses and ground deformation modelling have been performed during the shallow dislocation phases that have allowed the magma uprising (Fig. 2).

For each episode the cumulative seismic moment M_o was calculated released during dike emplacement that can be estimated using local magnitudes M_L and duration magnitudes M_d provided by data collected by the different networks (Fig. 3; Tab. 1).

The seismic moment M_o was obtained by using the Giampiccolo et al. (2007) relationship for the Mt. Etna earthquakes:

$$\mathrm{Log}(M_o) = (17.60 \pm 0.37) + (1.12 \pm 0.10)*M_L \quad (1)$$

where M_L is the local magnitude of each event. For the events before 2005 we converted M_d in M_L by using the Tuvè et al. (2015) relation:

$$M_L = 1.164\ (\pm 0.011) * M_d - 0.337\ (\pm 0.020) \quad (2)$$

The geodetic moment (M_G) for a planar source has been calculated using the relationship:

$$M_G = \mu * \Delta V \quad (3)$$

(e.g. Aki & Richards, 1980), where μ is the shear modulus and ΔV the opening crack volume.

We assumed a shear modulus of 10^{10} Nm^2 and we considered a percentage error related to modelled crack dimensions errors obtained from the deformation data inversions. Seismic and geodetic parameters for each episode are reported in Tab. 1.

- The first studied case is the 17-23 March 1981 eruption; it was characterized by a lateral 7 km long eruptive fissure that propagated, trending SSE to NNW, on the NW sector of the volcano (Kieffer, 1982). EDM and levelling data were modelled by Bonaccorso (1999). The resulting magma intrusion

155 was characterized by a double tensile crack, the former 1.36 km wide, 3.0 km long, with 5.2 meters of
156 opening and the latter 0.36 km wide, 6.6 km long, with 1.1 m of opening (Bonaccorso, 1999). This
157 eruption was preceded by a seismic swarm characterized by thousands of events recorded (Kieffer,
158 1982) with M_{max}=4.0 (Cosentino et al., 1981). Seismicity associated with the final intrusion phase (16-
159 17 March) comprised 1680 events (130 with M≥1.8) (Cosentino et al., 1981; unpublished UNICT
160 database).
161 - The 1989 eruption of Mt. Etna was characterized by the formation on 24 September of two fracture
162 systems, striking NE-SW and NNW-SSE respectively; both originating from the SE Crater (Frazzetta
163 & Lanzafame, 1990). The NE-SW fractures were characterized by magma effusive activity, whereas
164 the NNW-SSE fracture propagated until October, 3 for a length of 7 km, without eruptive associated
165 phenomena.
166 Ground deformation (Bonaccorso & Davis, 1993) and magnetic (Del Negro & Ferrucci, 1998) data
167 related to the NNW-SSE fracture have been interpreted as due to the emplacement of a shallow magma
168 dike, departing from the summit craters area towards the southern flank.
169 EDM and tilt data inversion produced a modelled dike 1.3 km wide, 0.8 long, 1.0 km depth, with 1.0
170 meters of opening. We considered the earthquakes recorded between September, 30 (05:00 UT) and
171 October, 3 (02:00 UT) a total of 642 events of magnitude (M_d) ranging from 1.0 to 2.9 (AA.VV.,
172 1989).
173 The 1991-93 was one of the longest in duration and volumetrically significant eruptions occurring on
174 Mt. Etna over the last 300 years. The eruption started from a fracture system originating at the base of
175 the SEC and propagated to the SSE down to 2200 meters elevation along the western wall of the Valle
176 del Bove. The eruption was characterized by a low-explosive activity, producing a lava field of about
177 7.6 km^2, with a total volume of outpoured magma of about 235 x 10^6 m^3 (Calvari et al. 1994).
178 A shallow source 0.8 km wide, 3.6 long crack with 2.8 meters of opening was inferred through an
179 analytical inversion performed by using EDM, GPS horizontal variations, three vertical maximum
180 changes and tilt (Bonaccorso et al, 1996).
181 The intrusive phase was accompanied by a seismic swarm of 197 recorded events (Patanè et al., 1994;
182 CNR-IIV, 1992) that occurred between 01:47 and 18:41 UT on December 14, 1991 (Bonaccorso et al.,
183 1996).
184 -The 2001 flank eruption (17 July - 9 August) occurred from several eruptive fissures. From summit
185 fractures the eruptions originated from the lateral draining of the central conduit system; However the

main eruptive episode occurred at the 2100 vent, where the forceful upraising of an eccentric dike below the south flank caused intense seismicity and ground deformation.

The magma was not drained from the central conduit system, but ascended vertically from a reservoir that had likely been emplaced within the sedimentary substratum (Benchke & Neri, 2001).

The 2001 eruption was preceded by a very strong seismic swarm that started 4 days before the eruption. 2694 earthquakes of magnitude (M_d) ranging from 1.0 to 3.9 occurred from 12 July until the end of the eruption (9 August), but the large majority (2645 events) occurred before the onset of lava emission on 17 July (Patanè et al., 2003).

Modelling of the deformation changes (Bonaccorso et al., 2002) infers a nearly N-S oriented vertical tensile crack 2 km long and 2.5 km high, with an opening of ca 3.5 m, located in the area on the upper southern flank, equivalent to a geodetic moment of $M_G = 1.77 \times 10^{17}$ Nm (Tab. 1).

Conversely, Puglisi et al. (2008) and Bonforte et al. (2009) have inverted discrete GPS datasets obtaining a shallower source, an opening of about 2 m, obtaining a M_G estimate of 8.7-8.9 x 10^{16} Nm (Tab. 1).

-The 2002-2003 eruption was characterized by both a vertical uprising dike in the upper southern flank (2002S), and another intrusion propagating radially in the NE flank, along the NE rift (2002NE).The onset of the 2002-2003 eruption during the night of 26 October 2002 was marked by an increase in the seismicity (starting at 20:25 UT) composed of more than 300 events with M_d>1. During the first 4 hours, seismicity took place in the southern-upper part of the volcano; subsequently, a clear migration of the earthquake location from summit craters area toward the NE Rift was observed which accompanied the NE flank intrusion for about 20 hours (Aloisi et al., 2006)

We considered the seismic moments for the two dike intrusions, obtaining 7.17 x 10^{14}Nm for the 2002S (56 events with M_{max}=2.7) and 1.89 x 10^{16}Nm for the 2002NE (252 events, M_{max}=4.2).

Aloisi et al., (2003) interpreted the observed ground deformation as consistent with a composite mechanism characterized by: i) a vertical uprising dike in the upper southern flank (2002S) 1.6 km long and 1.8 km high, with an opening of ca. 1.5 m (M_G = 4.3±0.8 x 10^{16}Nm) and ii) a lateral intrusion propagating into the north-eastern rift (2002 NE) 6.6 km long and 4.6 km high, with an opening of 1.0m (M_G = 2.2 x 10^{17}Nm). The 2002S intrusion was emplaced in the same pathway of 2001 eruption.

Currenti et al. (2007) proposed for the 2002NE an integrated approach based on the use of genetic algorithms whose results gave a M_G = 2.98 x 10^{16}Nm with an error of 25%.

-The 2008-09 eruption was characterized by the formation of a dry fracture field on the northern flank, and a lateral eruptive fissure on the upper eastern flank. It was accompanied by a strong seismic swarm

218 which started on May 13, 2008 at 08:40 (GMT). More than 200 events were recorded until 15:00, with
219 the main-shock of M=3.9 at 10:07. The earthquakes were localized in the north-eastern area of the
220 summit and from the 09:30 to 11:00 they showed a migration towards North which was interpreted as
221 an attempt of a shallower intrusion towards this sector (Patanè, 2008), producing a dry (not eruptive)
222 fracture field.
223 The intrusion was divided into two phases: the first represents an ascending vertical dike-like intrusion
224 and the second an attempt of the magma to penetrate laterally toward the north. The first dike intruded
225 in the high southern flank and the following eruptive fissure, while the lateral intrusion in the northern
226 flank stopped without lava emission, but induced a dry fracture field (Aloisi et al., 2009; Bonaccorso et
227 al., 2011). The two cracks modelled by Aloisi et al. (2009) furnish an overall M_G of 2.69 x 10^{16} Nm.
228 Currenti et al. (2011), by using DInSAR data, continuous GPS data and numerical modelling
229 procedures, inferred a complex and realistic deformation model with a volumetric expansion of crustal
230 rocks of about 5.3×10^6 m^3.
231
232 **4.0 Discussion and conclusions**
233 Table 1 reports the values (12) corresponding to 7 cases of dike sources modelled that comprises three
234 different models for the 2001 and 2002NE and two for 2002S and 2008.
235 Seismic/geodetic moment ratio (M_o/M_G) expresses the proportion of the stress energy accumulated
236 through deformation of the crust that is released by seismic events and may also be expressed as
237 seismic efficiency (*e*) if multiplied by 100 and expressed in per cent.
238 In particular, we obtained for the 1981, 1991-93 and 2002NE lateral episodes similar low moment
239 ratios, with values between 0.040 and 0.063 (Fig. 3 Tab. 1). The highest values, (0.25-0.50) have been
240 obtained for the 2001 while the 2008 eruption showed intermedia values (0.128-0.25). The 1989,
241 which represent an intrusive episode without eruption, showed a value of 0.174.
242 The values obtained, ranging from 0.017 to 0.5 ($1.7\% \leq e \leq 50\%$) are similar to that of other volcanic
243 areas. Very low values are seen in the Afar area of Ethiopia, Krafla and Eyjafjallajökullin in Iceland, A
244 value up to 0.55 is found for the 2007 intrusion at Gelai, Tanzania and 0.40 for the Izu Islands, Japan
245 and Hengill, Iceland (Calais et al., 2008; Baer et al., 2008; Toda et al., 2002; Pedersen, 2007).
246 Therefore, moment ratio may vary over several orders of magnitude, since seismicity associated with
247 magma movements is dependent on several factors, such as background regional stresses, geological
248 and tectonic setting of the intruded area (the background seismicity rate) (Pedersen et al., 2007).

These factors could be considered almost constant in a restricted area, such as Mt. Etna. Here, however, we have obtained a wide M_o/M_G variability, suggesting that the mechanism of the impeding eruptions may have an important role. We noted that:

- The lowest values (0.017-0.023) were obtained for the vertical 2002S dike intrusion that occurred in the southern area following the already fractured and weakened path of the 2001 intrusion. This fact could have favoured an easier and faster dike emplacement with a very low level of associated seismicity (Aloisi et al., 2003; 2006).
- For the 1981, 1991-93 and 2002 NE lateral eruptions the moment ratios have similar low values comprises between 0.040 and 0.063. This means that only about 5% of the stress energy accumulated with ground deformation is released in seismicity. This low seismic efficiency indicates that most of the strain change induced by dikes intrusion does not lead to brittle rupture of rock.
- The 2008 eruption showed values ranging from 0.128 (Currenti et al., 2011) to 0.25 (Aloisi et al., 2009). This episode was recognized as having a complex mechanism with two dikes one of which propagated laterally in the northern flank and arrested without lava emission (Aloisi et al., 2009; Bonaccorso et al., 2011).
- For the 1989 a moment ratio of 0.174, we obtained, suggests that the dike intruded for several days, causing a moderate/high seismicity, until it arrested without eruption.
- Finally, the 2001 vertical dike intrusion showed the highest values (0.5 or 0.25 according to the different models). The intrusion ascended directly from a deeper reservoir to the surface, forcefully opening a new path. Consequently, a large seismic energy release affected the volcano body for several days.

Overall on Mt. Etna the obtained moment ratios seem to have a relationship with the intrusive process type: low values for lateral eruptions, higher for vertical eccentric intrusions, whose uprising is prevented by geology and tectonic barriers.

An impeded intrusion needs more time to reach the surface and is accompanied by a larger seismicity, as is testified by the relationship between M_o/M_G and time (fig. 4).

Comparing moment ratio with dike intrusion duration we obtained the following linear best fit law:

281 $M_o/M_G = 0.0032t - 0.0058$ (4)

282

283 where t is the intrusion time expressed in hours with a correlation coefficient R^2=0.83.

284

285 By using the (3) we obtain:

286

287 $\Delta V = M_o/[\mu*(0.0032t - 0.0058)]$ (5)

288

289 The intruded volumes obtained by using equation (5) are shown in Table 1. The results obtained for the
290 2001 event volume (1.22E+07 m^3) falls right between the values obtained by three previous authors.
291 During hours that follow the beginning of a co-intrusive seismic swarm, the (4) relationship may
292 represent a useful tool for a simple and quick forecasting of the eruption onset (if we know M_o/M_G) and
293 intruding magma volumes (by using M_o). However, even if exist examples of deformation data
294 inversion in real time (e.g. Zhan et al., 2017) at present a M_G value in real-time is not available.
295 Instead, by using the (5) relationship is possible to obtain a rough but very fast estimation of the
296 intruded volumes and therefore the magnitude of the on-going volcanic process. Nevertheless, the 2008
297 eruption does not follow the relation, evidencing its peculiar intrusive process with high seismic
298 releases (probably linked to the intrusion attempt towards North) in a short time (in the light of the
299 successive fast eruptive intrusion to East).

300

301 **Acknowledgements**

302 We want to thank Páll Einarsson and an anonymous reviewer for their comments that lead to
303 substantial improvements to the manuscript. Alexandra Cooper and Suzanne Vickery are kindly
304 acknowledged for the revision of the English text.

305

306

307 **References**

308 AA. VV., 1989. Rapporto attività Etna Settembre–Ottobre 1989. Istituto Internazionale di Vulcanologia
309 Catania.
310 Allard, P., Behncke, B., D'Amico, S., Neri M., Gambino S., 2006. Mount Etna 1993–2005: Anatomy
311 of an evolving eruptive cycle Earth Science Review, 78, 85-114.

312 Aloisi, M., Bonaccorso, A., Gambino, S., Mattia, M., Puglisi, G., 2003. Etna 2002 eruption imaged
313 from continuous tilt and GPS data. Geophys. Res. Lett., 30, 23, 2214 10.1029/2003GL018896.
314 Aloisi, M., Bonaccorso, A., Gambino, S. 2006. Imaging compositive dike propagation (Etna, 2002
315 case). J. Geophys. Res., 111, B06404, doi: 10.1029/2005JB003908.
316 Aloisi, M., Bonaccorso, A., Cannavò, F., Gambino, S., Mattia, M., Puglisi, G., Boschi E., 2009. A new
317 dyke intrusion style for the Mount Etna May 2008 eruption modelled through continuous tilt and
318 GPS data. Terra Nova, 21, 316–321.
319 Aloisi, M. Mattia, M., Ferlito, C., Palano, M., Bruno, V., Cannavò F., 2011. Imaging the multi-level
320 magma reservoir at Mt. Etna Volcano (Italy). Geophys. Res. Lett., 38, L16306.
321 Aki, K., Richards, P.G., 1980. Quantitative Seismology: Theory andMethods. W.H. Freeman, New
322 York. pp. 932.
323 Baer, G., Hamiel, Y., Shamir, G., Nof R., 2008. Evolution of a magma-driven earthquake swarm and
324 triggering of the nearby Oldoinyo Lengai eruption, as resolved by InSAR, ground observations
325 and elastic modeling, East African Rift, 2007, Earth. Planet. Sci. Lett., 272, 339–352.
326 Behncke B., Neri, M., 2003. The July-August 2001 eruption of Mt. Etna (Sicily). Bull. Volcanol. 65,
327 461-476, doi: 10.1007/s00445–003–0274–1.
328 Bonaccorso, A., Davis, P.M. 1993. Dislocation of the 1989 dyke intrusion into the flank of Mount
329 Etna, Sicily. J. Geophys. Res. 98, 4261–4268.
330 Bonaccorso, A., Ferrucci, F., Patanè, D., Villari, L., 1996. Fast deformation processes and eruptive
331 activity at Mt. Etna (Italy). J. Geophys. Res.101, 17467–17480.
332 Bonaccorso A., Gambino S., 1997. Impulsive tilt variations on Mount Etna (1990-93), Tectonophysics,
333 270, 1-2, 115-125.
334 Bonaccorso, A., 1999. The March 1981 Mt. Etna eruption inferred through ground deformation
335 modelling. Physics of the Earth and Planetary Interiors, 112, 125-136
336 Bonaccorso, A., Aloisi M., Mattia M., 2002. Dike emplacement forerunning the Etna July 2001
337 eruption modeled through continuous tilt and GPS data. Geophys. Res. Lett., 29, 13, 1624,
338 10.1029/2001GL014397
339 Bonaccorso, A., A. Bonforte, S. Calvari, C. Del Negro, G. Di Grazia, G. Ganci, M. Neri, A. Vicari,
340 Boschi E., 2011. The initial phases of the 2008–2009 Mount Etna eruption: A multidisciplinary
341 approach for hazard assessment, J. Geophys. Res., 116, B03203, doi:10.1029/2010JB007906.
342 Bonforte A, Gambino S, Neri M., 2009. Intrusion of eccentric dikes: The case of the 2001 eruption and
343 its role in the dynamics of Mt. Etna volcano. Tectonophysics, 471, 1-2, 78-86.

344 Calais, E., et al., 2008. Strain accommodation by slow slip and dyking in a youthful continental rift,
345 East Africa, Nature, 456, 783–787, doi:10.1038/nature07478.
346 Calvari, S., Coltelli, M., Neri, M., Pompilio M. Scribano V., 1994. The 1991-1993 Etna eruption:
347 chronology and lava flow-field evolution. Acta Vulcanologica, 4, 1-14.
348 CNR-IIV, 1992. The current state of Mt. Etna Volcano – December 1991. Monthly report in the
349 framework of the activities coordinated by the GNV, IIV, Catania, Italy.
350 Cosentino, M., R. Cristofolini, M. Ferri, G. Lombardo,G. Patanè, R. Romano, A. Viglianisi, Villari P.,
351 1981. L'eruzione dell'Etna del 17–23 Marzo 1981. Rapporto preliminare, Rend. Soc. Geol. It.,
352 4(3), 249–252.
353 Currenti G., Del Negro, c., Fortuna, L., Ganci G., 2007. Integrated inversion of ground deformation and
354 magnetic data at Etna volcano using a genetic algorithm technique. Annals of Geophysics, 50, 1,
355 21-30. ISSN 2037-416X.
356 Currenti G, Napoli R, Del Negro C., 2011. Toward a realistic deformation model of the 2008 magmatic
357 intrusion at Etna from combined DInSAR and GPS observations. Earth Planet Sci Lett 312:22–
358 27. doi:10.1016/j.epsl.2011.09.058
359 Del Negro, C., Ferrucci, F., 1998. Magnetic history of a dike on Mount Etna (Sicily), Geophys. J. Int.
360 133,45 I-458.
361 Ferro A., Gambino S., Panepinto S., Falzone G., Laudani G. Ducarme, B., 2011. High precision tilt
362 observation at Mt. Etna Volcano, Italy. Acta Geophysica, 59, 3, 618-632.
363 Frazzetta, G., Lanzafame, G., 1990. The NE and SE fracture systems, in: Mt Etna the 1989 eruption,
364 edited by F. Barberi, B. Bertagnini, P. Landi, pp. 23-29.
365 Gambino S., G. Falzone, A. Ferro, Laudani G., 2014. Volcanic processes detected by tiltmeters: a
366 review of experience on Sicilian volcanoes, J. Volcanol. Geotherm. Res. 271, 43-54, 2014.
367 Giampiccolo, E., S. D'Amico, D. Patanè, Gresta S., 2007. Attenuation and source parameters of
368 shallow micro-earthquakes at Mt. Etna Volcano, Italy, Bull. Seismol. Soc. Am., 97, 184–197,
369 doi:10.1785/0120050252.
370 Gresta S., Patanè D., 1987. Review of seismological studies at Mount Etna. Pure Appl. Geophys. 125,
371 951–970.
372 Kieffer, G., 1982. L'éruption du 17 au 22 Mars 1981 de l'Etna: Sa signification dans l'évolution
373 actuelle du volcan, Géol. Méditerr., 9, 59 – 67.
374 Lo Giudice, E., Patanè, G., Rasà, R., Romano, R., 1982. The structural framework of Mt. Etna. Mem.
375 Soc. Geol. It., 23 125-158.

376 Neri, M., V. Acocella, B. Behncke, V. Maiolino, A. Ursino, Velardita R., 2005. Contrasting triggering
377 mechanisms of the 2001 and 2002 – 2003eruptions of Mount Etna (Italy), J. Volc. Geotherm.
378 Res., 144, 235 –255.
379 Obrizzo, F., Pingue, F., Troise, C., De Natale, G., 2001. Coseismic displacements and creeping along
380 Pernicana fault (Mt. Etna) in the last seventeen years: a detailed study of a structure on a volcano.
381 J. Volc. Geotherm. Res. 9, 109–131.
382 Okada, Y., 1985. Surface deformation due to shear and tensile fault in half-space, Bull. Seismol. Soc.
383 Am., 75, 1135-1154.
384 Patané, D., Privtera, E., Ferrucci, F., Gresta, S., 1994. Seismic activity leading to the 1991-1993
385 eruption of Mt. Etna and its implications, Acta Vulcanologica 4, 47-55.
386 Patanè D., et al., 2003. Seismological constraints for the dike emplacement of July-August 2001 lateral
387 eruption at Mt. Etna volcano, Italy. Ann. Geophys., 46, 599-608.
388 Patanè D., Cocina O., Falsaperla S., Privitera E., Spampinato S., 2004. Mt. Etna Volcano: a
389 seismological framework. In: S. Calvari, A. Bonaccorso, M. Coltelli, C. Del Negro and S.
390 Falsaperla (Eds.), The Mt. Etna Volcano. AGU, Washington, D.C., 147–165.
391 Patanè, D., 2008. Quadro di sintesi e aggiornamento al 19 Maggio 2008 sullo stato di attività sismica
392 dell'Etna, INGV internal report WKRSM20080519, http://www.ct.ingv.it/Etna2007/main.htm.
393 Pedersen R., Sigmundsson, F. Einarsoon P., 2007. Controlling factors on earthquake swarms associated
394 with magmatic intrusions; Constraints from Iceland J. Volc. Geoth. Res. 162, 73–80.
395 Puglisi, G., A. Bonforte, A. Ferretti, F. Guglielmino, M. Palano, Prati C., 2008. Dynamics of Mount
396 Etna before, during, and after the July–August 2001 eruption inferred from GPS and differential
397 synthetic aperture radar interferometry data, J. Geophys. Res., 113, B06405.
398 Toda, S., Stein, R.S., Sagiya T., 2002. Evidence from the AD 2000 Izuislands earthquake swarm that
399 stressing rate governs seismicity. Nature 419, 58–61.
400 Tuvè T., D'Amico, S., Giampiccolo E., 2015. A new M_d-ML relationship for Mt. Etna earthquakes
401 (Italy). Ann. Geophys. 58, 6, doi:10.4401/ag-6830S0657.
402 Zhan, Y., Gregg, P. M., Chaussard, E., Aoki, Y., 2017. Sequential Assimilation of Volcanic
403 Monitoring Data to Quantify Eruption Potential: Application to Kerinci Volcano, Sumatra. Front.
404 Earth Sci., doi.org/10.3389/feart.2017.00108.
405
406
407

Captions

Fig. 1 - Map showing the Mt. Etna surface faults the sliding sector (dashed line). Top inset map shows the main regional fault systems: MF is Messina–Fiumefreddo, ME is Malta Escarpment, and ATL is Aeolian–Tindari–Letojanni (a). Mt. Etna seismic and geodetic networks (b).

Fig. 2 - Map showing the Mt. Etna eruptive dike intrusive sources obtained by ground deformation data modelling.

Fig. 3 - Seismic to geodetic moment ratio for each modelled eruptive dike intrusion. Grey area evidences the similar values for the 1981, 1991-93 and 2002 NE lateral eruptions.

Fig. 4 - Seismic/geodetic moment ratio versus time. The linear law gives an empirical relation to estimate intruding magma volumes.

Figures

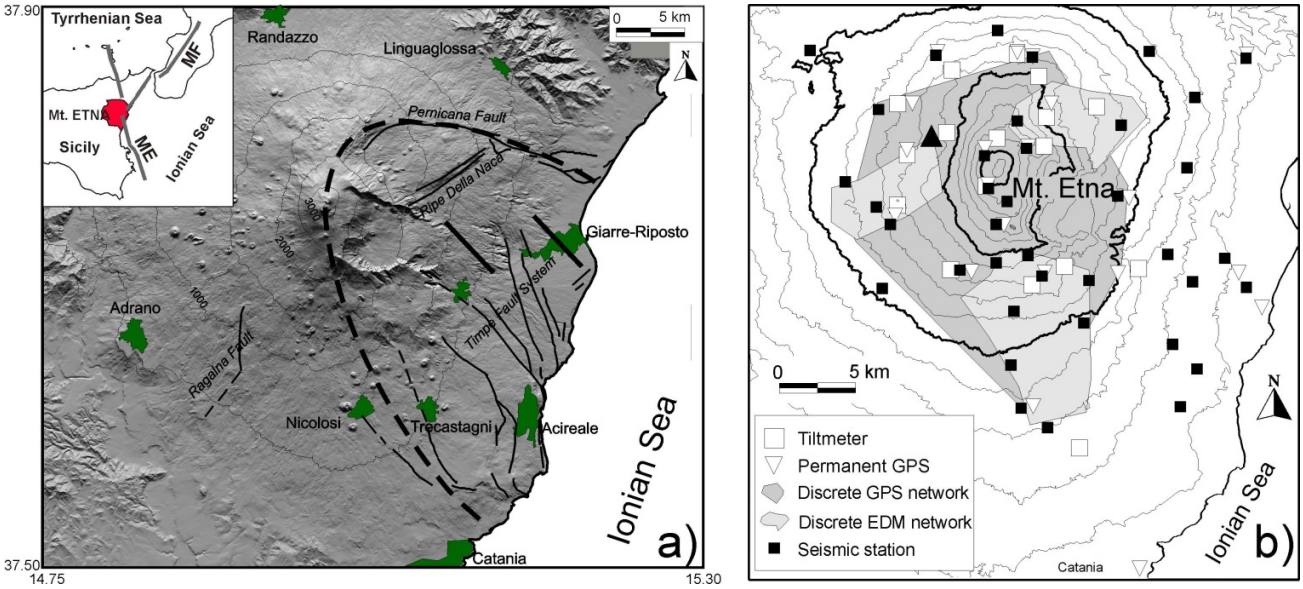

Figure 1

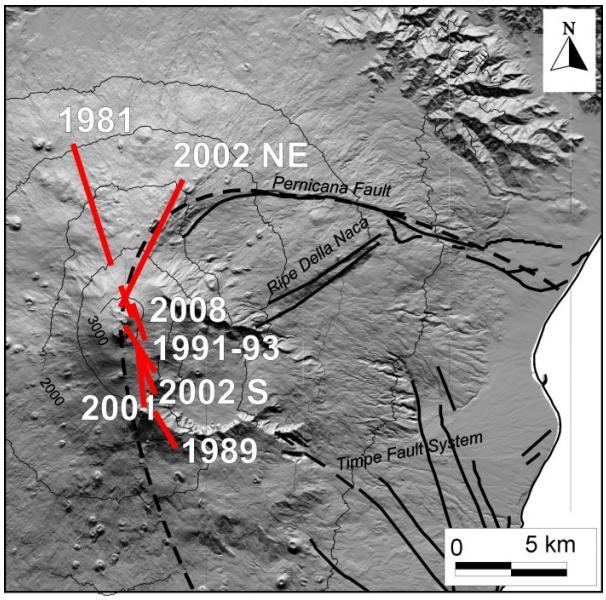

Figure 2

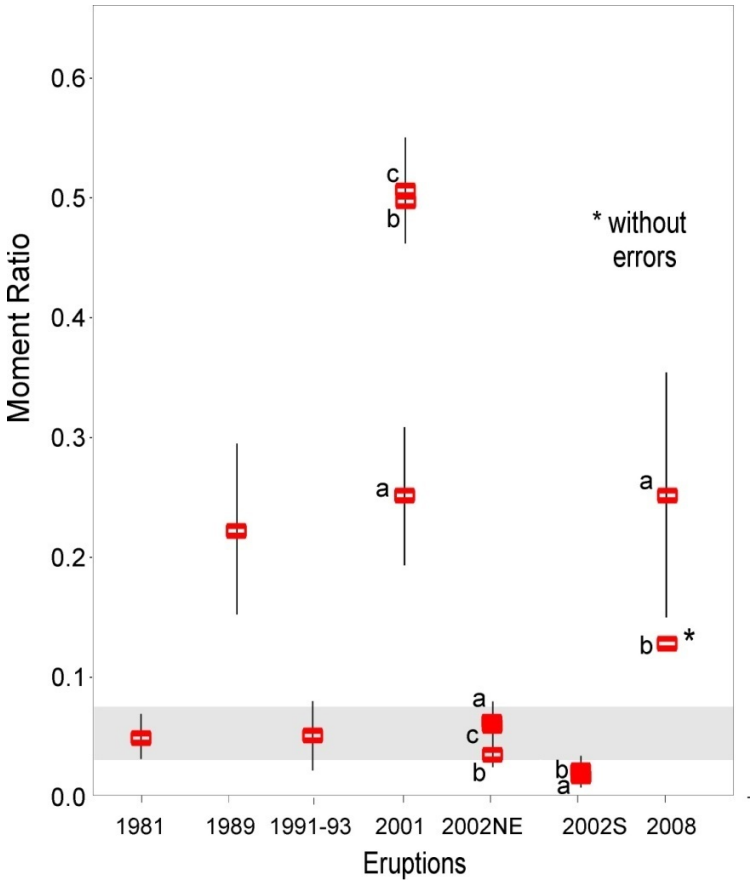

Figure3

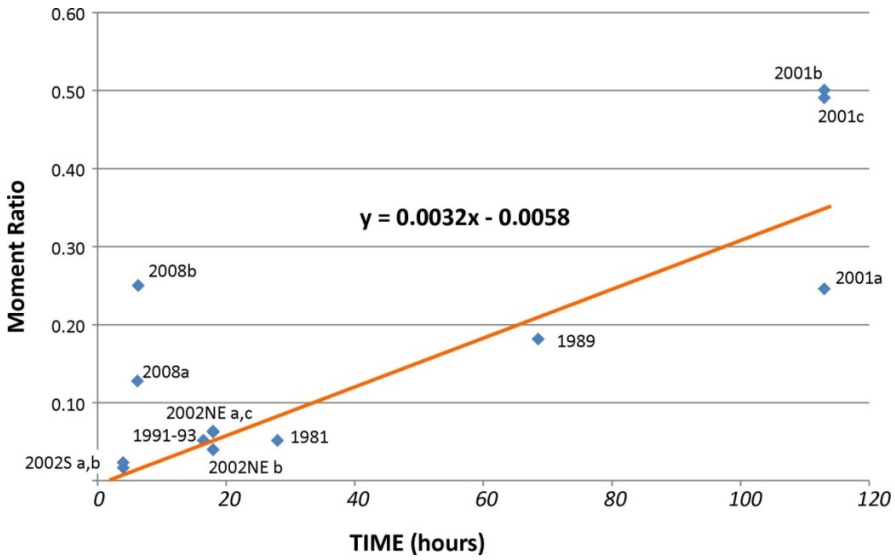

Fig. 4

Table 1 -Parameters of different eruptive dike modeled from ground deformation data and associated cumulative seismic moment released during the intrusion. Int. dur: Intrusion duration; Mod. volume was obtained by modeling; Rel. volume from (4) relationship.

Eruptive episode	Type	Int. Dur. hours	Model reference	Dike depth (m. a.s.l.)	M_G (N/m)	Error %	Mo (N/m)	Moment Ratio	Mod. Volume m3	Rel. Volume m3
1981	Lateral	26	*Bonaccorso, 1999*	1800	2.38E+17	23.1	1.20E+16	**0.050**	2.38E+07	1.58E+07
1989	Stopped	68	*Bonaccorso & Davis, 1993*	1100	1.01E+16	14.9	1.76E+15	**0.174**	1.01E+06	8.31E+05
1991-93	Lateral	17	*Bonaccorso et al., 1996*	800	8.00E+16	21.3	4.09E+15	**0.051**	8.00E+06	8.42E+06
2001	Eccentric	113	*Bonaccorso et al., 2002*	250	1.77E+17	21.0	4.35E+16	**0.246**	1.77E+07	1.22E+07
		113	*Puglisi et al., 2008*		8.87E+16	7.8	4.35E+16	**0.490**	8.87E+06	1.22E+07
		113	*Bonforte et al., 2009*		8.69E+16	8.0	4.35E+16	**0.501**	8.69E+06	1.22E+07
2002 S	Eccentric	4	*Aloisi et al., 2003*	500	4.32E+16	26.0	7.17E+14	**0.017**	4.32E+06	8.66E+06
		4	*Aloisi et al., 2006*		3.10E+16	25.9	7.17E+14	**0.023**	3.10E+06	8.66E+06
2002 NE	Lateral	18	*Aloisi et al., 2003*	1500	3.04E+17	20.0	1.89E+16	**0.062**	3.04E+07	3.65E+07
		18	*Aloisi et al., 2006*		4.77E+17	30.0	1.89E+16	**0.040**	4.77E+07	3.65E+07
		18	*Currenti et al., 2007*		2.98E+17	25.0	1.89E+16	**0.063**	2.98E+07	3.65E+07
2008	Lateral/stopped	6	*Aloisi et al., 2009*	1850	2.69E+16	24.1	6.80E+15	**0.253**	2.69E+06	5.07E+07
		6	*Currenti et al., 2011*		5.30E+16	no error	6.80E+15	**0.128**	5.30E+06	5.07E+07